JOURNAL OF MATERIALS SCIENCE 23 (1988) 2325–2338

Fatigue crack growth behaviour of tungsten carbide–cobalt hardmetals

P. R. FRY*, G. G. GARRETT‡
Department of Metallurgy and Materials Engineering, University of the Witwatersrand, Johannesburg, South Africa

Fatigue crack propagation studies have been carried out on a range of WC–Co hardmetals of varying cobalt content and grain size using a constant-stress intensity factor double torsion test specimen geometry. Results have confirmed the marked influence of mean stress (through K_{max}), which is interpreted in terms of "static modes" of fracture occurring in conjunction with a "true" fatigue process, the existence of which can be rationalized through the absence of any frequency effect. Dramatic increases in fatigue crack growth rate are found as K_{max} approaches that value of stress intensity factor ($\geqslant \sim 0.9 K_{IC}$) for which static crack growth under monotonic load (or "static fatigue") occurs in these materials. Lower crack growth rates, however, produce fractographic features indistinguishable from those resulting from "fast" fracture. These observations, and the important effect of increasing mean free path of the cobalt binder in reducing fatigue crack growth rate, can reasonably be explained through a consideration of the mechanism of fatigue crack advance through ligament rupture of the cobalt binder at the tip of a propagating crack.

1. Introduction

For many engineering materials fatigue crack growth plays a dominant role in determining component life. In general terms this is also true for many applications of WC–Co hardmetals, which are used almost exclusively in variable loading situations (Table I).

For many applications, however, the criteria for alloy selection may not include fatigue life. Hardness, wear resistance, toughness, elevated temperature deformation properties and yield strength, for example, may all supersede the requirement for resistance to fatigue.

Fatigue initiated fracture, however, is undoubtedly a major cause of failure of many components manufactured from WC–Co. The variation in life to failure of high-pressure magnification anvils used in the synthetic diamond industry is one prime example indicating that cyclic crack growth is a mechanism for failure, and indeed this problem provided the motivation for the work reported in this paper.

Slow crack growth under variable loading conditions can occur by one of two mechanisms. In many materials, and particularly in metals, "true" fatigue occurs wherein crack growth is primarily dependent on the range of crack tip stress intensity that occurs under cyclic loading, often with some influence of mean stress intensity level. However, so-called "static fatigue" can also occur whereby the crack front extends only at a rate controlled by the stress intensity at the crack tip and the time for which the crack is loaded under that stress intensity; in this latter case, under cyclic loading, the mechanism of crack advance is not one of fatigue at all but simply a "static" growth mechanism, the same as that which occurs during crack growth under monotonic loading, manifesting itself under cyclic loading.

WC–Co hardmetals are low toughness, nominally "brittle" materials that behave in many ways like the ceramics for which the static mode of slow crack growth is a recognized phenomenon [1, 2]. However, with the presence of the ductile cobalt "binder" phase, "true" fatigue must be seen as a possible mechanism contributing to failure.

In the work described here, fatigue crack growth rate data have been measured for a selection of WC–Co hardmetals at different load ranges with the objective both of documenting conventional da/dN against ΔK data and of obtaining an insight into the possible mechanism(s) of fatigue crack propagation in this material system. In particular, it was considered important, and necessary, to attempt to verify conclusively whether or not crack growth under variable loading occurred by true fatigue.

2. Material description

Tungsten carbide–cobalt hardmetal is a composite whose two constituents, having widely differing properties, contribute to one of the most technically successful combinations currently in general engineering usage. A wide variety of hardmetal grades can be obtained by varying the proportions of hard, brittle tungsten carbide grains and relatively soft, ductile cobalt-rich binder.

The respective properties of the two phases and the

* *Present address:* Winders, Barlow and Morrison, 99 Leichhardt Street, Spring Hill, Brisbane, Queensland 4000, Australia.
‡ *Present address:* National Institute for Materials Research, CSIR, Pretoria, South Africa.

0022–2461/88 $03.00 + .12

TABLE I Typical applications of WC–Co components

Composition ranges		Grain structure	Application categories		Typical applications
WC	Co		Abrasion	Shock	
97–98	2–3	fine	extreme	none	wire-drawing dies, shot-blast nozzles, plug gauges, machine parts
95–97	3–5	fine or medium	very severe	very low	drawing and compacting dies, machines parts, lathe centres,
92–95	5–8	fine			bushes, thread guides, pen balls
94–95	5–6	medium	severe	low	masonry and glass drills, scribers, tyre studs, rolls, woodworking routers, machine
90–92	8–10	fine			parts, mechanical seals
90–94	6–10	medium	medium	medium	extrusion dies, rolls, scrapers, work-rest blades, mandrels, forming blades
92–95	5–8	coarse	moderate to	medium to	twist and guide rolls, plane irons and other woodworking
89–90	10–14	fine or medium	medium	severe	cutters, grinding mill components, punching and blanking dies
87–92	8–13	coarse	moderate	severe	heading and forming dies,
70–85	15–30	medium or coarse			anvils, crushers, hammers

current state-of-knowledge concerning the structure–property relationships of the composite material have recently been extensively reviewed by Exner [3]. This review does not cover all the mechanical properties of WC–Co, however, and other literature is available to provide further details on fatigue [4–10], and fracture toughness [11–17].

Central to the description of the behaviour of WC–Co hardmetals is the definition of a microstructural parameter that can uniquely identify any combination of grain size and composition. Two parameters have been widely used for this purpose, with the so-called "true mean free path" now generally beginning to replace the "nominal mean free path". Both of these parameters recognize that the cobalt binder exists as a continuous network of varying thickness. The true mean free path assumes, however, that some cobalt-free contiguous WC–WC boundaries exist in the microstructure, contrary to the nominal mean free path definition which assumes a binder layer between all the grains.

Thus the nominal mean free path is defined as

$$\lambda_{nom} = \frac{\text{(vol. fraction cobalt)(mean WC grain size)}}{\text{(1 - vol. fraction cobalt)}} = \frac{f_{Co}\bar{d}}{(1 - f_{Co})}$$

The so-called true mean free path, however, includes a factor accounting for the contiguity (C) of the WC–WC skeleton:

$$\lambda_{true} = \frac{\text{(vol. fraction cobalt)(mean WC grain size)}}{\text{(1 - vol. fraction cobalt)(1 - contiguity)}} = \frac{f_{Co}\bar{d}}{(1 - f_{Co})(1 - C)}$$

Here, contiguity is defined as the ratio of the carbide–carbide grain boundary area to the total surface area of the carbide grains [18–20].

These two mean free path parameters are particularly convenient to use because only the mean WC grain size needs to be measured by quantitative microscopy. The contiguity has been shown to have a unique relationship to the volume fraction of cobalt so that the work of previous researchers can be used to obtain C [21].

In the work reported here, several different hardmetals have been tested, as detailed in Table II, but many of the details of material behaviour have been determined on only one of the hardmetals (G10, see Fig. 1) and the behavioural trends confirmed on two or three of the others. The hardmetals chosen, having as they do different microstructural variables of grain

TABLE II Details of alloys tested

Alloy: Boart grade designation	Cobalt content (wt %)	Cobalt vol. fraction (f_{Co})	WC grain size, nominal	WC($\bar{d}$) measured (μm)	Contiguity	Nominal mean free path (μm)	True mean free path (μm)	Hardness, VPN (kg mm^{-2})	K_I (MN m$^{-3/2}$)
S6	6	0.101	fine	1.0	0.50	0.093	0.186	1541	8.2
S10	10	0.164	fine	1.1	0.36	0.216	0.338	1337	9.1
G6	6	0.101	coarse	2.9	0.50	0.327	0.654	1377	10.0
G10	10	0.164	coarse	3.1	0.36	0.608	0.950	1215	11.3
G15	15	0.237	coarse	3.5	0.25	1.090	1.453	1043	13.3
25E	25	0.370	coarse	3.2	0.13	1.882	2.163	798	15.7

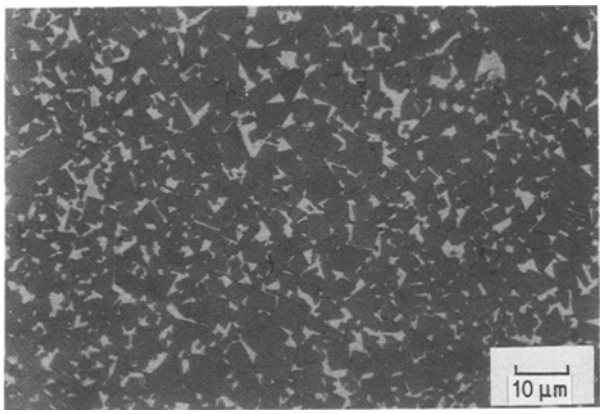

Figure 1 Representative microstructure of hardmetal G10, WC-10Co coarse grained × 1200.

size and cobalt content, have lead to a set of results covering a reasonable range of mean free path.

It is also relevant to note that the composition of the cobalt-rich binder phase, although not examined in detail in the present work, can have a considerable influence on mechanical properties; in particular, control of the carbon content is important in obtaining the required properties from WC–Co hardmetals. In the materials reported on here, magnetic saturation values were not measured but metallographic examination revealed that some free carbon was present in all grades.

The operational factors that have been investigated in fatigue are mean stress intensity factor, R ratio, amplitude of stress intensity factor range and frequency. The fatigue data produced have been presented in the form of conventional plots of crack growth rate against stress intensity factor range. For comparison, some limited tests on crack growth under monotonic loading were also undertaken.

3. Fatigue behaviour of tungsten carbide–cobalt hardmetals

A number of researchers have examined the fatigue behaviour of tungsten carbide–cobalt hardmetals, and some interesting differences emerge, as summarized in Table III. For example, it seems reasonably well established that increasing the cobalt content improves fatigue life, both in S–N type tests [4, 22] and crack propagation studies [9]. Work performed in compression, however, by Johanssen *et al.* [7], suggests precisely the opposite trend.

Several workers have, more recently, obtained conventional fatigue crack growth rate data for these materials (e.g. [8–11, 23, 24]) several of whom [8, 9] have used the double torsion specimen employed in this investigation. Evans and Linzer [8] were evidently the first to obtain measurable fatigue crack growth in WC–Co, although their experiments were aimed primarily at test development and not the determination of structure–property relationships in WC–Co.

The programme of study reported by Almond and Roebuck [10] regrettably only produced a single set of results (for one hardmetal). Lueth [9], on the other hand, gives crack growth rate data for a range of alloy compositions but without reporting the load range (R) ratio or mean stress intensity factor; in addition, Lueth indicates that his results fit an equation of the form $da/dN = C\Delta K^m$ yet his straight line data are plotted only semi-logarithmically.

Using a short rod technique, Viswanadham [11] has examined the effect of R ratio, up to 0.6, indicating an increase in growth rate with increasing R. He has also performed a limited study on the influence of frequency, showing that growth rate (da/dN) decreased by ~ 2 to 3 for an increase in frequency over the range 0.5 to 5 Hz. Evans and Linzer [8] also discuss the frequency effect, but without presenting any quantitative results; they show that the rate of change in specimen compliance, and therefore crack growth rate, with time, is strongly frequency dependent, implying that crack growth in fatigue takes place by a truly cyclic mechanism. This point will be examined further in this present paper, but it is interesting to note that Lueth [9] concludes, in contrast, that fatigue is not an active failure mechanism but rather that "static" crack growth occurring under cyclic-loading is dominant.

Lueth bases this assertion entirely on fractographic evidence that showed fatigue fracture surfaces to be identical to those produced by a continuously propagating crack; in his studies, fracture occurred predominantly in the cobalt binder phase with characteristic

TABLE III Summary of fatigue observations

Issue	Observations	
Effect of increasing cobalt content	Fatigue life increased. Kreimer [22], Miyake *et al.* [4], Lueth [9]	Fatigue life decreased. Johansson *et al.* [7]
Fatigue fracture surface	Ductile failure of binder i.e. same as fast fracture. Davies and Barhana [6], Lueth [9], Viswanadham [32]	Brittle failure of binder. Almond and Roebuck [10]
Mechanisms	Static effects. Lueth [9]	True cyclic effect. Almond and Roebuck [10], Evans and Linzer [8]
Fatigue limit or K_I threshold	Does exist. Kreimer [22], Lueth [9]	Does not exist. Miyake *et al.* [4], Davies and Barhana [6] Johansson *et al.* [7]

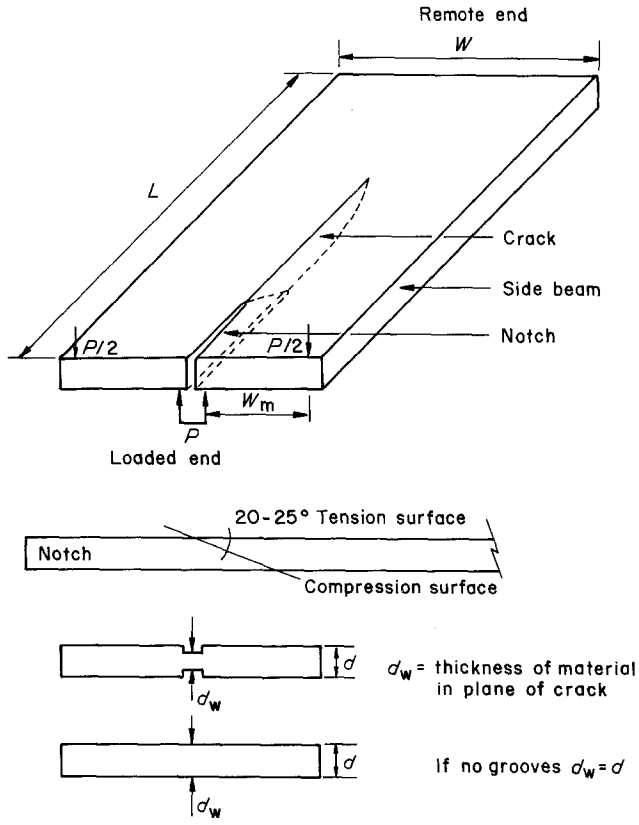

Figure 2 Diagram illustrating the basic geometry, dimensions and terminology used in the double torsion test.

ductile dimples. In contrast again, Almond and Roebuck [10] report that, in fatigue, the binder-phase regions fail with little plastic deformation by a fracture mode that is partly cleavage and is characterized by surface markings that are crystallographic in nature. They explain this observation in terms of cyclic stress-induced work hardening of the cobalt binder at a propagating crack tip.

In conclusion, therefore, there are a number of interesting anomalies requiring further investigation, as the experimental programme we have performed [25], and reported here, has attempted to do.

4. Experimental details

The most rational and widely used approach to the problem of obtaining accurate fatigue data which are not subject to the influences of variations due, for example, to the number of cycles to initiation, is the measurement of cyclic crack growth rate (da/dN) as a function of the operating stress intensity range (ΔK).

The data thus obtained not only precisely characterize the fatigue properties or the influence of, for example, mean stress level on the behaviour of the material under test, but also provide the necessary information for a fracture mechanics evaluation of a component's anticipated service performance.

Clearly an experimental technique had to be selected whereby the fatigue crack growth rate under a variety of load conditions could conveniently be measured in this material. For brittle materials, however, conventional fracture mechanics specimens are generally far from ideal because, with their low toughness, the stress intensity factor has to be very carefully controlled to prevent premature fast fracture. It is, therefore, preferable to use constant stress intensity factor geometries where the stress intensity factor is independent of the crack length.

There are a number of geometries available which fulfil this requirement, and these have been adequately reviewed elsewhere [26]. In particular the "double torsion" test specimen (Fig. 2) first proposed by Outwater and Jerry in 1966 [27], and since reviewed in some detail (e.g. [28–30]), has gained popularity in recent years and has been used extensively by various authors both to measure fracture toughness and to obtain slow crack growth data in brittle materials subjected to monotonic as well as fatigue loading. The major advantages are that the specimen geometry is relatively simple and easy to manufacture, and the corresponding analysis is supposedly straightforward with experiments being easy to perform. However, there are, unfortunately, a number of unresolved questions concerning the technique. These relate primarily to the validity of the stress intensity factor at the crack front and deal with parameters such as the position of the crack tip, the shape of the crack front, the effect of grooves, the dimensions of the specimen and interaction between the cracked surfaces [28, 30]. In addition, there has been no standardization of test procedure, and consequently a wide variety of methods and geometries have been employed. The authors have used a geometry which has been shown by other work to provide valid data [28].

The double torsion specimen consists essentially of a thin, flat rectangular plate with a starter notch cut into one end. The co-linear point loads applied at the notched end effectively cause propagation down the centre line of the specimen; however, load point misalignment influences the crack direction. The use of well-aligned samples with no centre groove (the

stress concentration effect of which is unknown) appears to be the ideal situation.

The mode I stress intensity at the crack tip, K_I, is given by [31, 32]:

$$K_I = PW_m \left[\frac{3}{Wd^3 d_w (1 - \nu)\varepsilon} \right]^{1/2}$$

where terms are defined in Fig. 2, and ν = Poisson's ratio, $\varepsilon = 1 - 0.6302t + 1.20te^{-\pi/t}$, and $t = 2d/W$. In this paper K will generally be used for K_I, for convenience. K_{Ic} will be used as the conventional designation for the fracture toughness.

Tests with this geometry in sintered WC–Co samples were carried out on a 50 kN capacity ESH universal servo-hydraulic testing machine. Continuous crack length measurement was essential, and this was performed using an optical travelling microscope and dye penetrant: the position of the crack tip was easily identified by smearing a thin layer of dye on the surface of the specimen while the fatigue load was being applied. (The dye selected was Magnaflux Spotcheck, Penetrant SKL-HF, a commercially available penetrant which meets various specifications such as ASME Section 5, Article 6, Paragraph T630. Crack growth tests were carried out under monotonic load using the dye and no measurable growth was measured until the applied stress intensity factor reached approximately $0.9\,K_{Ic}$. This result agreed with the results obtained by Osterstock [2] using double cantilever beam specimens in air. It was concluded, therefore, that the dye penetrant was not contributing in any way to time-dependent crack growth.)

Six different hardmetals were tested covering a range of grain sizes and cobalt content (see Table II). Grade G10 was used as the "base line" material as it represents approximately the middle of the range of carbide grain size and cobalt binder content. Tests on other hardmetals were used to confirm data and trends observed in the G10 grade. The test samples, none of which contained grooves, were of dimensions 200 mm × 75 mm × 6 mm. They were notched using a spark erosion machine; the end of the notch was sharpened using a diamond wafering blade. Fatigue precracking was carried out at low loads, possible because of the notch shape (initially small d_w therefore high K), and if it was apparent that the crack was not straight, suitable adjustment of the specimen alignment could be made to alter the crack direction and bring it to the centre.

Crack growth under monotonic loading has been reported by Osterstock [2] using the double cantilever beam technique. His results show that static crack growth only occurs at stress intensity factors close to the fracture toughness, i.e. $K \gtrsim 0.9\,K_{IC}$. In the current work static crack growth tests were also carried out on two hardmetals, measuring crack length directly. The "load relaxation" technique described by various authors [28, 29, 33] was not successful and did not produce any meaningful results. Instead, static crack growth data were obtained by applying and maintaining loads which were known to be less than the critical load for a period of time, after which the crack growth was measured using dye penetrant. In this way complete V–K curves for two hardmetals were produced.

A wide range of fatigue crack growth rate tests was undertaken, the objectives being: to determine whether or not true fatigue exists in WC–Co hardmetals; to characterize fatigue in this range of hardmetals; and to obtain information which would lead to an understanding of the mechanisms of fatigue. To this end crack growth rates were measured in a variety of compositions under a range of load conditions, altering variables such as mean stress intensity factor, R ratio and cyclic frequency. In the test work carried out, a frequency of 5 Hz was used throughout, except where frequency effects were being investigated.

Two tests can confirm whether "true" fatigue occurs and does not simply consist of static crack growth mechanisms operating during cyclic stressing. The first concerns the influence of frequency, because if growth rate (da/dN) is by true fatigue it will be dependent on the number of cycles, i.e. independent of frequency (assuming environmental influences in laboratory air and room temperatures in this material can be neglected). If, however, static mechanisms control the crack growth process the growth rate (da/dN) will be time dependent, and therefore dependent on frequency, with an apparent reduction in da/dN as frequency increases.

Secondly, Evans and co-workers [34, 35], by measuring the static crack growth rate under monotonic loading and the fatigue growth rate with the factor $\Delta K/K_{(av)}$ constant, have shown mathematically that if there is no true fatigue the slope of the crack growth rate with respect to time, da/dt plotted against K_{av} or K, is the same for both monotonic and cyclic loading.

5. Results

In the fatigue testing programme reported here, the effects of mean stress intensity factor (K_{av}), stress intensity factor amplitude (ΔK), R-ratio, frequency, carbide grain size ($\bar{d}$) and cobalt content have been examined.

In the first instance, a series of tests were performed at low R ratios (i.e. $P_{min}/P_{max} \leqslant 0.1$), appropriate to the industrial application of many WC–Co components such as drill bits, dies, anvils, rolls, etc., where the load is either "on" or "off". (Here obviously $R = 0$, but to avoid load-point impacting, R-ratios in the range 0.03 to 0.08 were actually used.) From the results, shown in Fig. 3, it is apparent that an increase in cobalt content results in improved fatigue resistance, in agreement with the work of Lueth [8]; increasing the carbide grain size also produces a similar effect. The results shown in Fig. 3 represent results from several specimens with data points taken at different positions on each specimen. The scatter bands indicate the full range of the results. These trends correspond with an increasing mean free path (Fig. 4a), although interestingly enough the value of the exponent m in the typical Paris growth rate equation also decreased with increasing mean free path (Fig. 4b).

It has been found that normalizing the ΔK values with respect to the fracture toughness (K_{Ic}) of the alloy

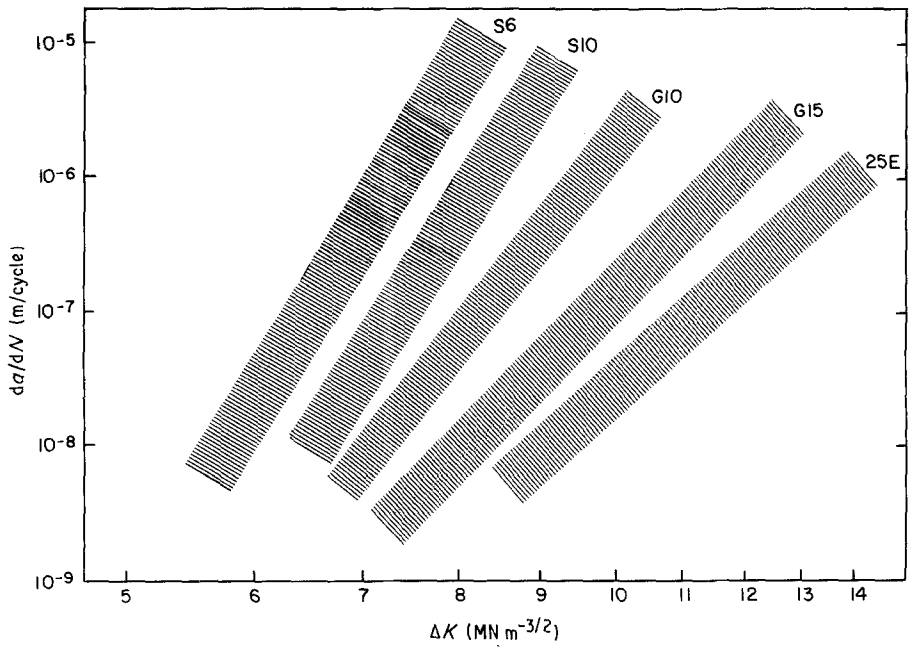

Figure 3 Influence of composition and grain size on fatigue crack growth behaviour in tungsten carbide–cobalt hardmetals. R = 0.04 to 0.08, frequency = 5 Hz. 56, WC–6Co fine grained, m = 19.7. S10, WC–10Co fine grained, m = 19.2. G6, WC–6Co coarse grained, m = 15.5. G10, WC–10Co coarse grained, m = 15.2. G15, WC–15Co coarse grained, m = 14.2. 25E, WC–25Co coarse grained, m = 10.9.

puts all the data in a relatively narrow scatter band (Fig. 5a); in plotting m for $R \approx 0$ against K_{Ic}, as done by Knee and Plumbridge [24], an almost linear correlation is obtained (Fig. 5b).

The sensitivity of the exponent m to mean stress intensity factor (Fig. 6), was evaluated by examining the da/dN against ΔK relationship, in a given hardmetal, as a function of K_{av}, keeping K_{av} constant throughout each test, with ΔK increasing. Depending on the material these results indicate that, below a given value of K_{av}, m tends to become fairly constant (Fig. 6). However, a closer inspection of the load spectrum showed that, in fact, m starts to increase only when the K_{max} values approach $\simeq 0.9 K_{Ic}$, the regime of static crack growth under monotonic loading.

These data can readily be plotted to demonstrate, more conventionally, the effect of increasing R-ratio on fatigue crack propagation (Fig. 7). This illustrates R effects, but this is not particularly useful for mechanistic information or interpretation as both ΔK and K_{av}, for R constant, change. No stress intensity factor parameter remains constant.

In order to examine further the influence of mean stress intensity factor K_{av}, stress intensity factor range ΔK, and maximum stress intensity factor K_{max}, tests were conducted at constant ΔK with increasing K_{av}. The results so obtained, for alloys G10 and S10, are shown in Fig. 8.

The observation from the load spectrums used to obtain Fig. 6 is that m starts increasing when the peak stress intensity factor, K_{max}, is sufficiently large to enter the regime of time-dependent static crack growth under monotonic loading. This time-dependent growth (Fig. 9) should not be confused with static mechanisms of crack growth which occur in fatigue and contribute to the relatively high m values measured. This appears to be confirmed from Fig. 8, where both K_{av} and K_{max} are plotted, together with the corresponding static crack growth measurements and fracture toughness values determined for the two hardmetals under consideration. Thus a growth rate transition is in evidence where K_{max} (in fatigue) has a value greater than the minimum stress intensity factor required for static crack growth, under monotonic load (sometimes known as "static fatigue"). The high m values obtained and the mechanisms of crack growth are discussed in more detail in the next section.

In this work static crack growth under monotonic load was only measured to assist with explaining the increase in m values at high K_{max}. The results obtained on hardmetals S10 and G10 are shown in Fig. 9; these gave n values of 125 and 194, respectively. It is of interest to note that the measurements made confirm the results reported by Osterstock [2], i.e. that static crack growth under monotonic loading starts at around $0.9 K_{IC}$ with n values (where $V = AK^n$) in the range 125 to 200.

Fracture toughness values for the hardmetals were obtained by loading the pre-cracked DT specimens to failure at a ramp rate of 0.05 mm sec^{-1}. As we have reported elsewhere [23, 25], the fracture toughness of the series of hardmetals tested increases approximately linearly with mean free path, decreasing with increasing hardness (Table II), and thereby mirrors fatigue crack propagation resistance (Figs 4 and 5). The fracture toughness values measured are all below those determined by other investigators with respect to both hardness and mean free path. This difference may be due to the presence of free graphite in the material tested, but there must still be some doubt as to the validity of some precracking techniques used by other investigators.

The contribution of (time-dependent) static crack growth mechanisms to the rate of fatigue crack propagation can be determined, as previously mentioned, through an examination of the effect of frequency on

crack growth rate. In this instance, a useful "change-over" test technique was employed, whereby fatigue crack growth was monitored at a specific load range and frequency. Without changing any other test parameters, an order of magnitude frequency change permits unequivocal evaluation of the frequency effect. In this way, hardmetals S10, G10, G15 and 25E (see Table II) were tested at 0.5, 5 and 50 Hz.

In the ΔK ranges under test, there is no significant frequency effect on crack growth rate, da/dN; see for example the results on alloy G10 at 5 and 50 Hz (Fig. 10a). However, increasing the frequency from 5 to 50 Hz increases the crack growth rate with respect to time, da/dt, by a factor of 10 (Fig. 10b). This provides strong evidence for a fatigue mechanism that, unlike that in static crack growth, is not time dependent. However, further justification is needed to confirm this point unequivocally, particularly as the number of tests and frequency range examined is quite small. This point will be examined further in Section 6.

From an extensive fractographic examination of the resulting fatigue fracture surfaces, and in comparison with the fracture morphology resulting from fast

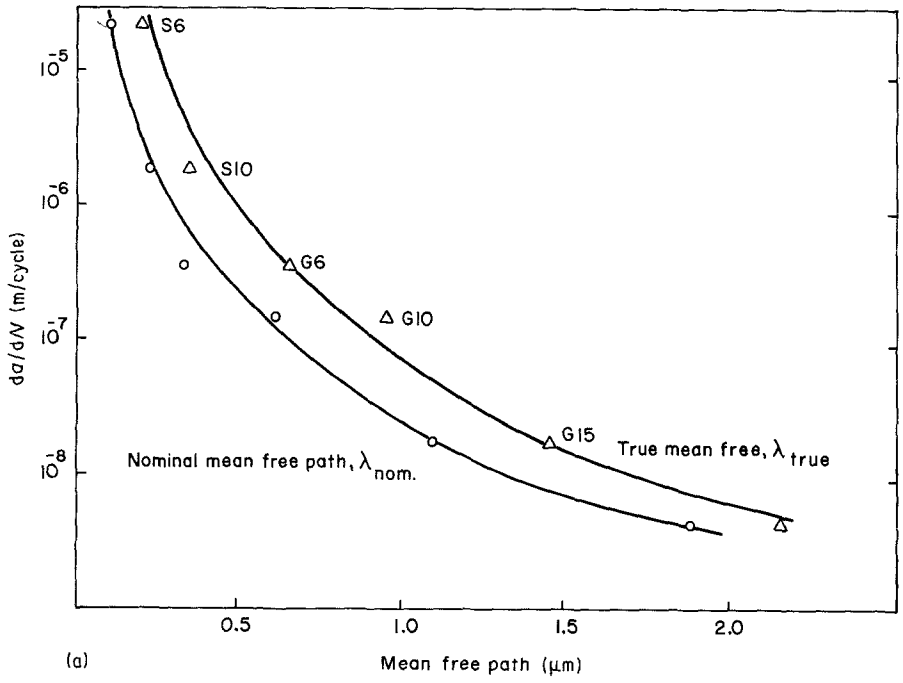

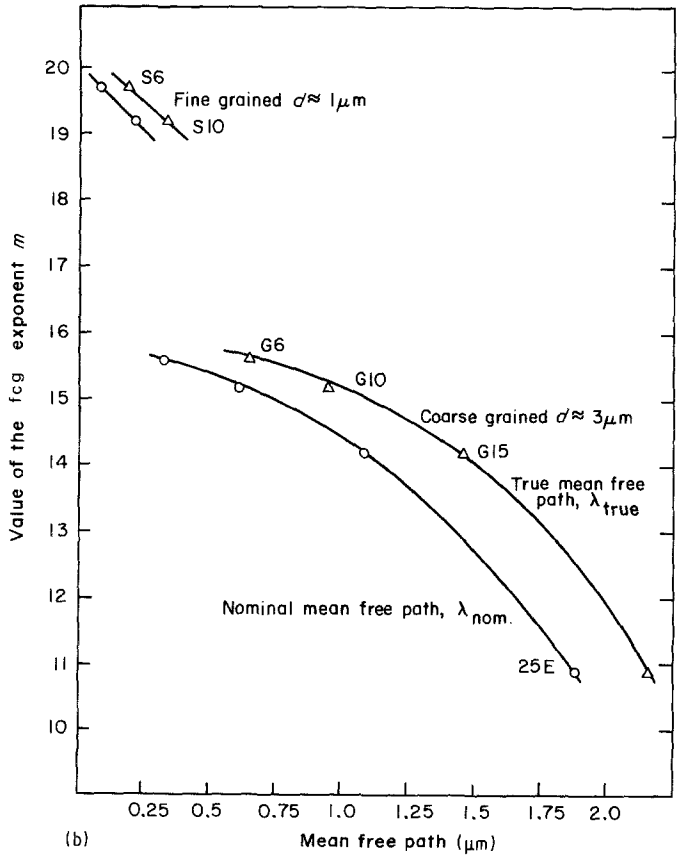

Figure 4 Variation of (a) fatigue crack growth rate with mean free path for a selected stress intensity range, $\Delta K = 8.5\,\mathrm{MN\,m^{-3/2}}$ ($R = 0.04$ to 0.08), and (b) the fatigue crack growth exponent m with mean free path ($R = 0.04$ to 0.08).

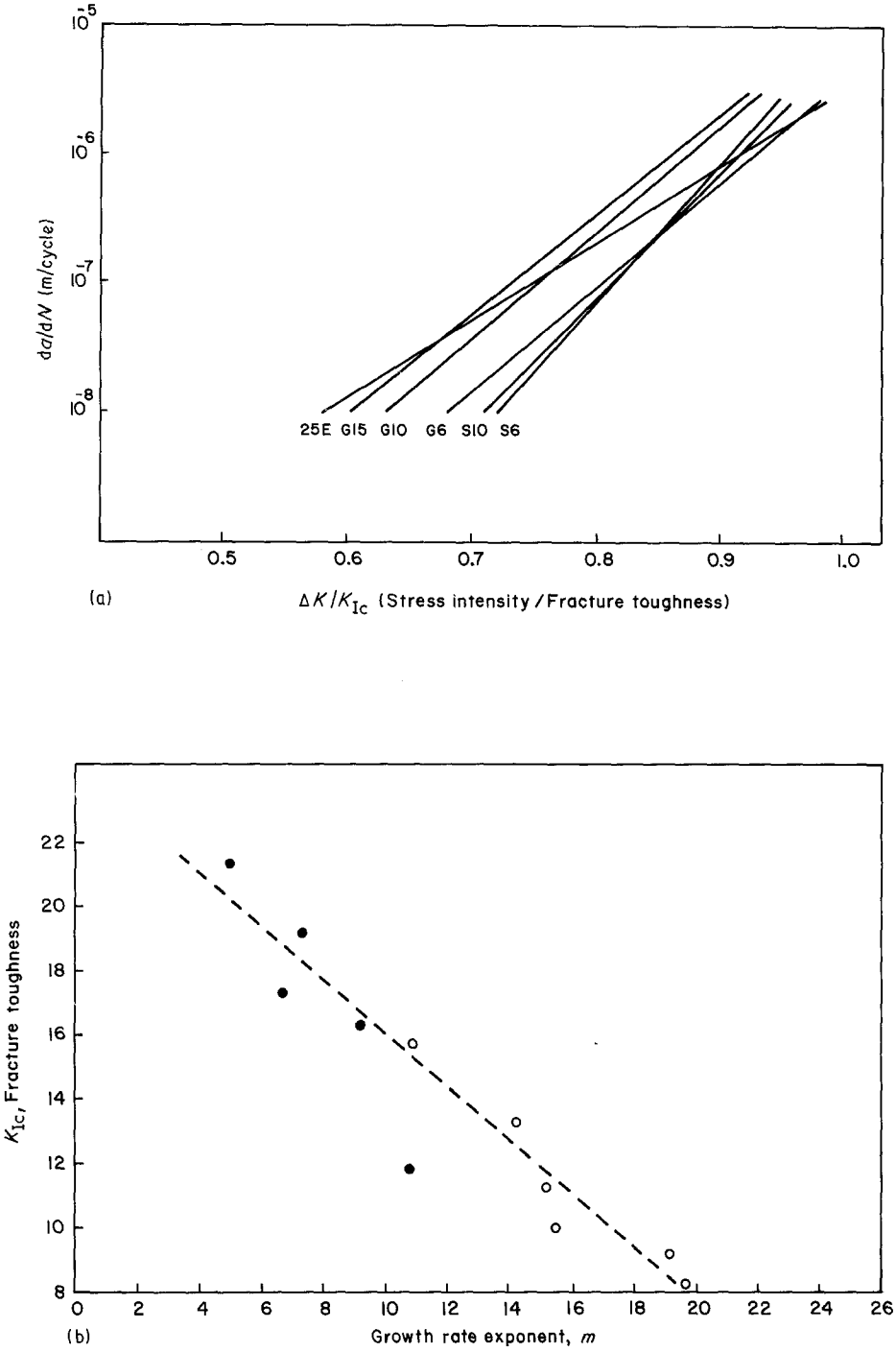

Figure 5 (a) Fatigue crack growth rate plotted against stress intensity range normalized with respect to fracture toughness (R = 0.04 to 0.08). (b) Inverse relationship between fatigue crack growth rate exponent, m, and fracture toughness, K_{Ic} (established for $R \simeq 0.1$). (○) Present work, (●) [24].

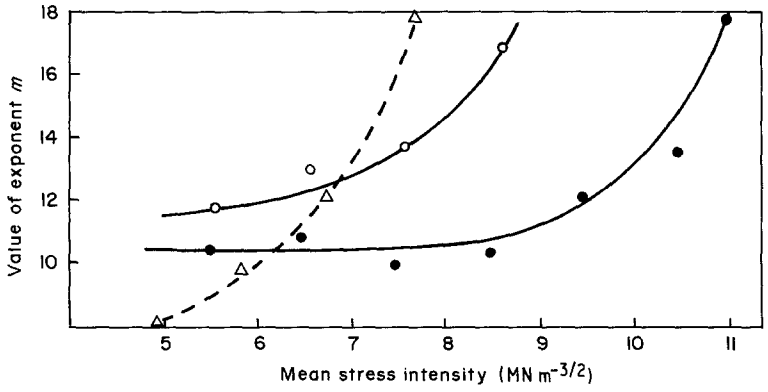

Figure 6 The influence of mean stress intensity, during fatigue crack propagation on the growth rate exponent. (△) Hardmetal S10 = WC–10Co, find grained; (○) hardmetal G6 = WC–6Co, coarse grained; (●) hardmetal G10 = WC–10Co, coarse grained.

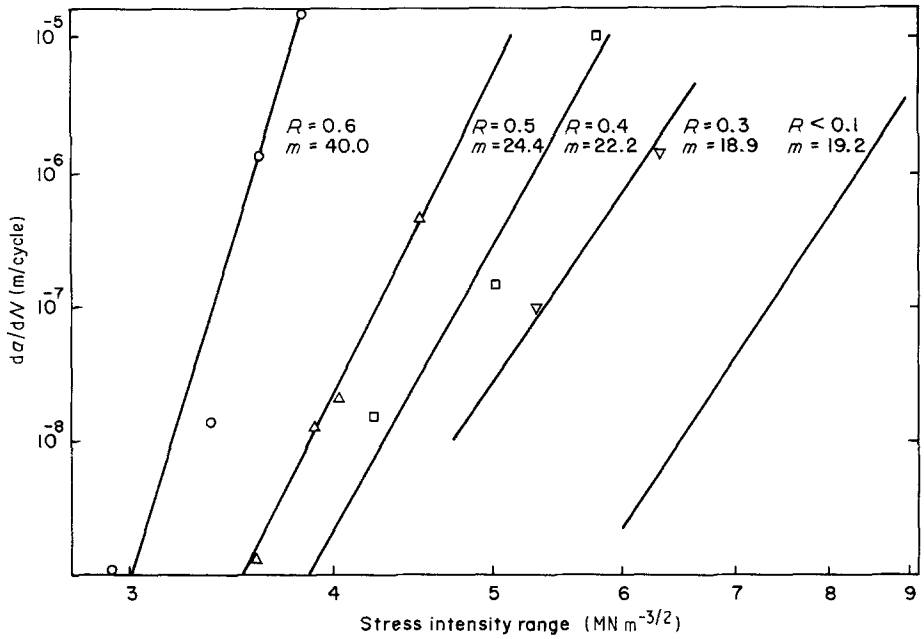

Figure 7 Fatigue crack growth rates at constant R ratios, alloy S10, WC–10Co fine grained.

fracture (from fracture toughness testing), it was evident that there are no distinguishable differences between the fatigue and fast fracture surfaces (Fig. 11), in any of the hardmetals tested, over the wide range of R-values studied [25]. In both situations, fracture is primarily intergranular, with ductile rupture occurring in the cobalt binder phase, although cleavage fracture of the carbide grains is also frequently in evidence (Fig. 12). (On an experimental note, it has been found to be very important to ensure extremely careful sample preparation and fracture surface protection in order to achieve good fractographic quality: rapid surface degradation takes place in the absence of appropriate precautions during the cutting of samples for mounting in the SEM.)

6. Discussion

Both the monotonic and cyclic crack growth rates determined in this investigation are slightly greater than results reported in the literature for similar compositions [2, 8–10]. However, the absolute differences are small and certainly the effects of variables such as cobalt content and mean stress are in full agreement with the observations of other workers, and therefore a sound basis for further discussion.

In summary: fatigue crack growth rates obey a Paris-type growth rate "law" of the form $da/dN = C\Delta K^m$, but are markedly influenced by mean stress level; growth rates decrease with increasing mean free path of the cobalt binder; m values lie in the range 10 to 20 but increase with decreasing mean free path or increasing mean stress; dramatic increases in fatigue crack growth rate occur as K_{max} approaches the K value ($\gtrsim 0.9\,K_{IC}$) for which monotonic crack growth occurs; da/dN is insensitive to frequency over the range 0.5 to 50 Hz tests; fatigue and fast fracture surfaces are indistinguishable.

Values of m in the range 2 to 4 are, of course, widely reported for ductile materials where continuum growth occurs and crack extension per cycle is likely to vary as some function of the crack opening displacement, involving a ΔK^2 dependence of crack growth rate. The mechanism of crack advance here is largely dependent on the crack tip slip processes, with crack growth dominated by the cyclic stress intensity factor range, ΔK. Higher values of crack growth rate exponent have, however, been satisfactorily explained (and fractographically supported) by the occurrence of "static" modes of fracture, such as brittle cleavage or microvoid coalescence, contributing to the overall rate of crack propagation by effectively being superimposed on the "conventional" fatigue process (e.g. [36, 37]). These static modes are not to be confused with static crack growth mechanisms which occur under monotonic loading, such as stress corrosion or hydrogen cracking, and are typically manifested by a mean stress dependence of fatigue crack growth rate and high m values. These static fracture modes are normally a function of the maximum crack tip stress intensity (K_{max}); the apparent mean stress sensitivity, through K_{av}, in fact only reflects the influence of K_{max} so that K_{av} is not, in itself, a controlling parameter.

The results and observations on fatigue crack propagation in WC–Co summarized above, suggest that both cyclic and static modes of fracture contribute to fatigue crack growth. Time-dependent crack growth does not appear to operate in fatigue, because da/dN is essentially independent of frequency, as previously mentioned. There is, however, evidence to show that time-dependent static crack extension contributes to fatigue crack growth as K_{max} exceeds $\sim 0.9\,K_{IC}$ and some frequency dependence of da/dN might, therefore, be expected were tests to be carried out at these high levels of K_{max}.

Along this line, Evans and co-workers [34, 35] have described, mathematically, a useful method of deriving cyclic crack propagation data from static crack growth results, where the mechanistic origins of crack advance are identical, i.e. where cyclic effects produce

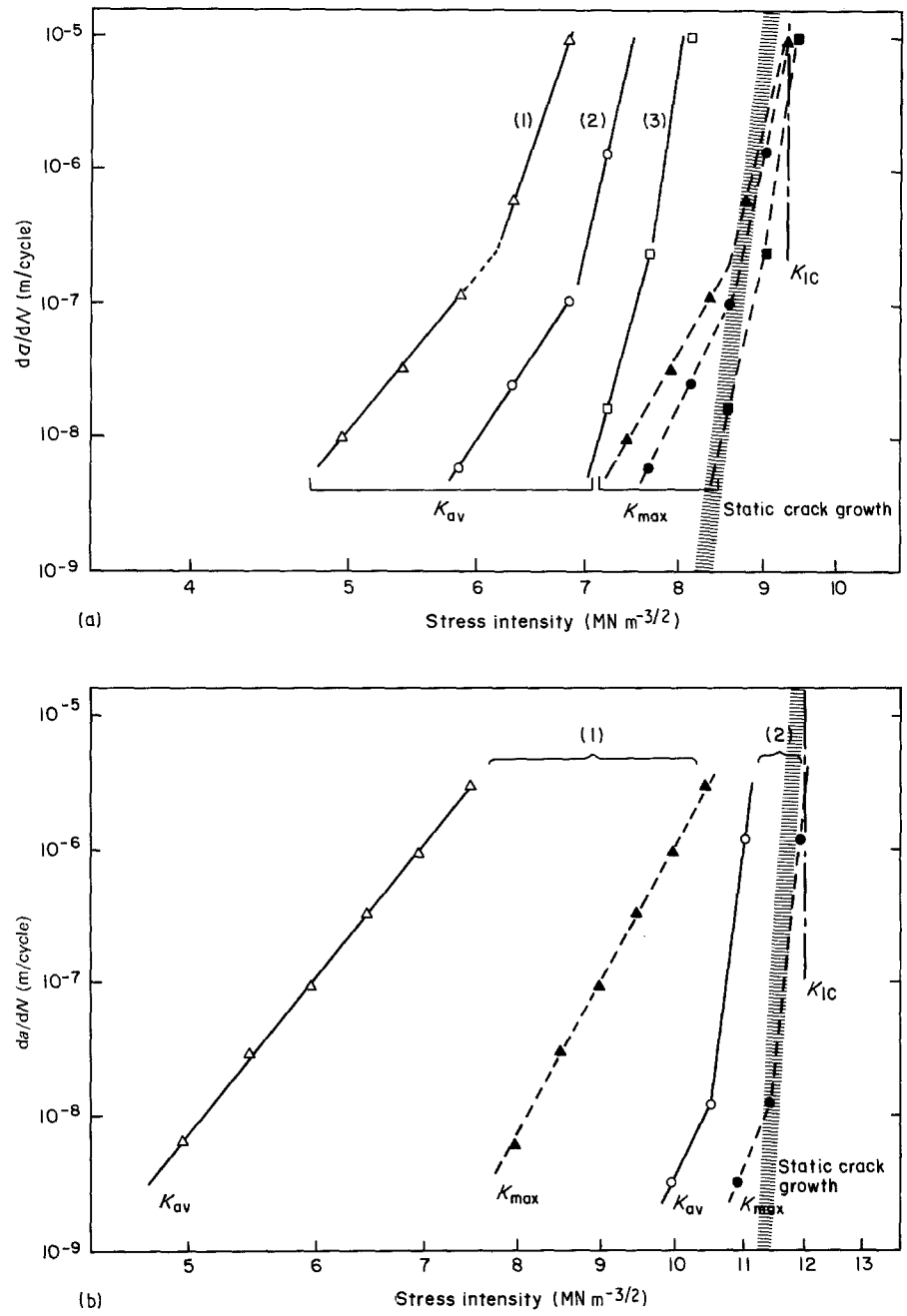

Figure 8 Fatigue crack growth rate data for constant ΔK, with mean stress intensity, K_{av}, increasing. These diagrams clearly illustrate the effect on crack growth when the maximum stress intensity reaches the static crack growth regime. (△, ○, □) Mean stress intensity. (▲, ●, ■) Maximum stress intensity. (a) Alloy S10, WC–10Co fine grained. ΔK_i = (1) 4.95 MN m$^{-3/2}$, (2) 3.60 MN m$^{-3/2}$, (3) 2.70 MN m$^{-3/2}$. (b) Alloy G10, WC–10Co coarse grained. ΔK_i = (1) 5.97 MN m$^{-3/2}$, (2) 1.99 MN m$^{-3/2}$.

no additional contribution to crack growth (as is the case for many ceramics, for example). The crack velocity at each point during a load cycle is, therefore, equal to the velocity as determined by monotonic loading, static crack growth measurements; for example, if the crack velocity at 7.5 MN m$^{-3/2}$ is 10^{-7} m sec^{-1} under static load, then during fatigue as K passes through the value 7.5 MN m$^{-3/2}$ the crack velocity at that instant will also be 10^{-7} m sec^{-1}. The net cyclic crack growth rate can therefore be predicted from monotonic measurements by integration of the cyclic stress intensity factors.

Evans' analysis shows that the fatigue data, plotted with $\Delta K/K_{av}$ constant, should then have the same slope as the static growth curve. For alloy G10, for example, the slopes obtained for three $\Delta K/K_{av}$ values of 0.8, 0.65, 0.5 are, respectively, 29.4, 26.8 and 24.6 [25]. In contrast, the corresponding monotonic slope is 194, confirming the conclusion implied by the (nil) frequency effect, that fatigue crack growth takes place by a "true" cyclic mechanism in this material.

In concluding this discussion, it is appropriate to consider briefly the mechanism by which fatigue cracks can grow in WC–Co hardmetals. Extensive fractographic observations (for example, as illustrated by Figs 11 and 12) tend to suggest a mechanism of crack advance along the lines of that illustrated schematically in Fig. 13. Thus, at any position, the crack front is likely to be rather poorly defined, with still intact cobalt ligaments spanning the crack behind regions of intergranular decohesion (by ductile rupture) and transgranular carbide fracture.

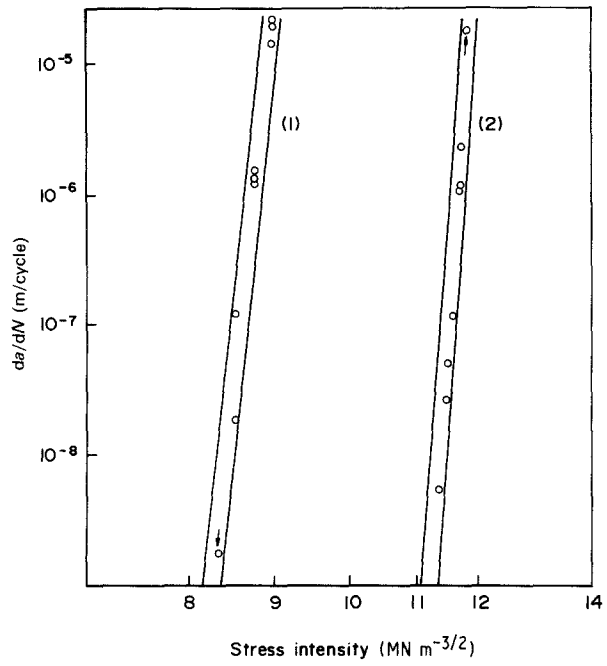

Figure 9 The influence of grain size and stress intensity factor on the time-dependent static crack growth behaviour of two tungsten carbide–cobalt hardmetals. (1) Alloy S10, WC–10Co fine grained, $n = 125$, $K_{Ic} = 9.17\,MN\,m^{-3/2}$. (2) Alloy G10, WC–10Co coarse grained, $n = 194$, $K_{Ic} = 11.85\,MN\,m^{-3/2}$.

For both fatigue crack propagation resistance and fracture toughness, the mean free path (the average binder layer thickness) has been shown to be of considerable importance (e.g. Fig. 5). Evans' model of the system [38] seems entirely appropriate, i.e. that of a relatively brittle carbide phase contained in a high ductility, high toughness binder, where the carbide grains impose triaxial constraint on the binder. The degree of constraint, and hence the local mechanical behaviour, depends on the binder layer thickness: where constraint is high the binder has high effective strength but limited ductility. As the binder layer thickness increases the constraint will decrease and ligament failure strain will increase, effectively increasing the inherent toughness of the composite.

In fatigue, there exists a combination of debonded grain boundaries, fractured grains and ruptured binder, and interspersed among these areas are ligaments of intact, but strained, cobalt binder (Fig. 13). The grain boundaries, the carbide grains and the highly constrained binder (small binder layer thickness) fail by the "static" modes of cleavage and microvoid coalescence. In fatigue the intact binder ligaments will be subject to alternating stresses which, due to crack opening, will be greatest in those ligaments subjected to the highest strain, i.e. those closest to the fully cracked material. As results have shown that stable fatigue crack growth does occur, with the crack advancing in successive individual or groups of cycles, some mechanism of cyclic damage must operate, but consistent with a fracture morphology more or less identical to that produced in conventional "fast" fracture.

Almond and Roebuck [10] have proposed a mechanism based on work hardening in which the binder ligaments become increasingly less ductile with each fatigue cycle. However, the development of work hardening is generally a strain-controlled process and can only increase if the strain on the ligament increases, i.e. if the crack advances, which is itself dependent on ligament rupture. Even taking into

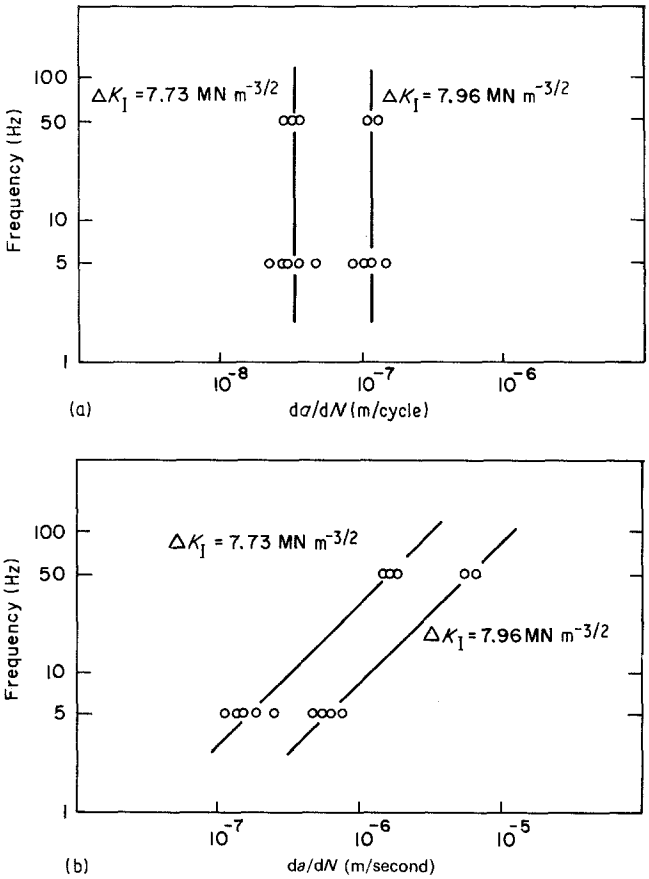

Figure 10 Variation in da/dN with test frequency in alloy G10, WC–10Co coarse grained, (a) indicating that there is no significant change in crack growth rate per cycle as frequency increases, and (b) illustrating the marked influence of frequency on crack growth rate with respect to time.

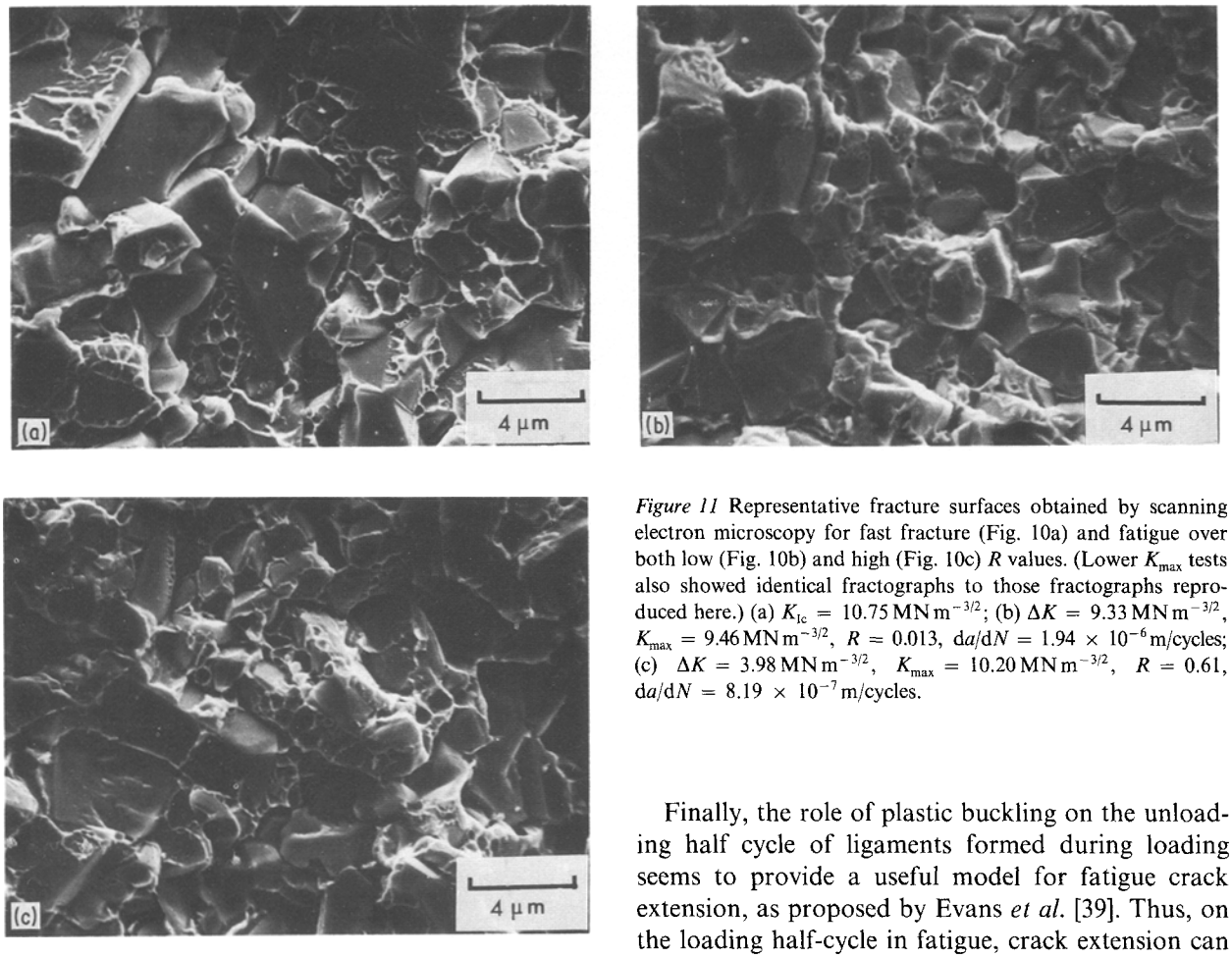

Figure 11 Representative fracture surfaces obtained by scanning electron microscopy for fast fracture (Fig. 10a) and fatigue over both low (Fig. 10b) and high (Fig. 10c) R values. (Lower K_{max} tests also showed identical fractographs to those fractographs reproduced here.) (a) $K_{Ic} = 10.75\,MN\,m^{-3/2}$; (b) $\Delta K = 9.33\,MN\,m^{-3/2}$, $K_{max} = 9.46\,MN\,m^{-3/2}$, $R = 0.013$, $da/dN = 1.94 \times 10^{-6}$ m/cycles; (c) $\Delta K = 3.98\,MN\,m^{-3/2}$, $K_{max} = 10.20\,MN\,m^{-3/2}$, $R = 0.61$, $da/dN = 8.19 \times 10^{-7}$ m/cycles.

account cyclic work hardening effects, such a mechanism does not offer an entirely adequate explanation of how crack advance actually takes place.

Along this line, however, consideration of each (plastically strained) ligament as a "microstructural" low cycle fatigue specimen, undergoing reasonably high plastic strains each cycle, would provide a reasonable interpretation for incremental crack advance. The magnitude of plastic strain experienced by each crack-bridging ligament will be a function of the crack tip opening displacement, and therefore on the applied stress intensity range, ΔK. No difference in fracture morphology would be anticipated because, similarly, no fractographic differences are normally observed between high strain, low-cycle fatigue failures and corresponding "fast" fracture surfaces. The K_{max} dependence of crack growth rate would be explained by static modes accompanying "pure" fatigue.

Alternatively (or even simultaneously), it is conceivable that stress cycling could cause the metastable fcc structure of the cobalt binder to undergo a stress-induced transformation to the room temperature stable hcp structure. As relatively little is known about the parameters that control this transformation, no precise mechanism can be proposed. However, if the percentage of binder phase which transforms increases with the number of cycles, as has been reported by Miyake *et al.* [4], then it is possible that the ligaments become increasingly less able to extend to the imposed crack tip strain, and rupture.

Finally, the role of plastic buckling on the unloading half cycle of ligaments formed during loading seems to provide a useful model for fatigue crack extension, as proposed by Evans *et al.* [39]. Thus, on the loading half-cycle in fatigue, crack extension can occur by static modes such as carbide grain cleavage or microvoid coalescence in the binder phase, with some ligaments being formed ahead of the crack tip but remaining intact as the peak stress in the cycle is reached. On unloading, many of these ligaments will buckle extensively, reducing their resistance to rupture on the following loading cycle.

The extent of crack advance through static modes is dependent on the maximum stress intensity, K_{max} [37], while buckling damage to the ligament will depend on the extent to which the crack closes, i.e. K_{min}. Thus both K_{max} and ΔK are also adequately accommodated in this explanation.

The decrease in m observed as the mean free path increases, means that the incremental crack advance per cycle is reduced. For a given crack tip opening, the binder ligaments will be thicker and more resistant to rupture either by alternating stress cycling (high strain, low cycle) and/or buckling-induced failure.

7. Conclusions

1. Fatigue crack growth rates have been measured in a series of tungsten carbide–cobalt hardmetals, utilizing a constant K, double torsion test specimen geometry. In agreement with other authors, the data are found to obey a conventional Paris growth "law" formulation with m values lying in the range 10 to 20.

2. Mean stress has a substantial influence on crack growth rate. This can be interpreted, through the influence on K_{max}, in terms of the effect of "static modes" occurring in conjunction with the fatigue process.

3. Dramatic increases in fatigue crack growth rate

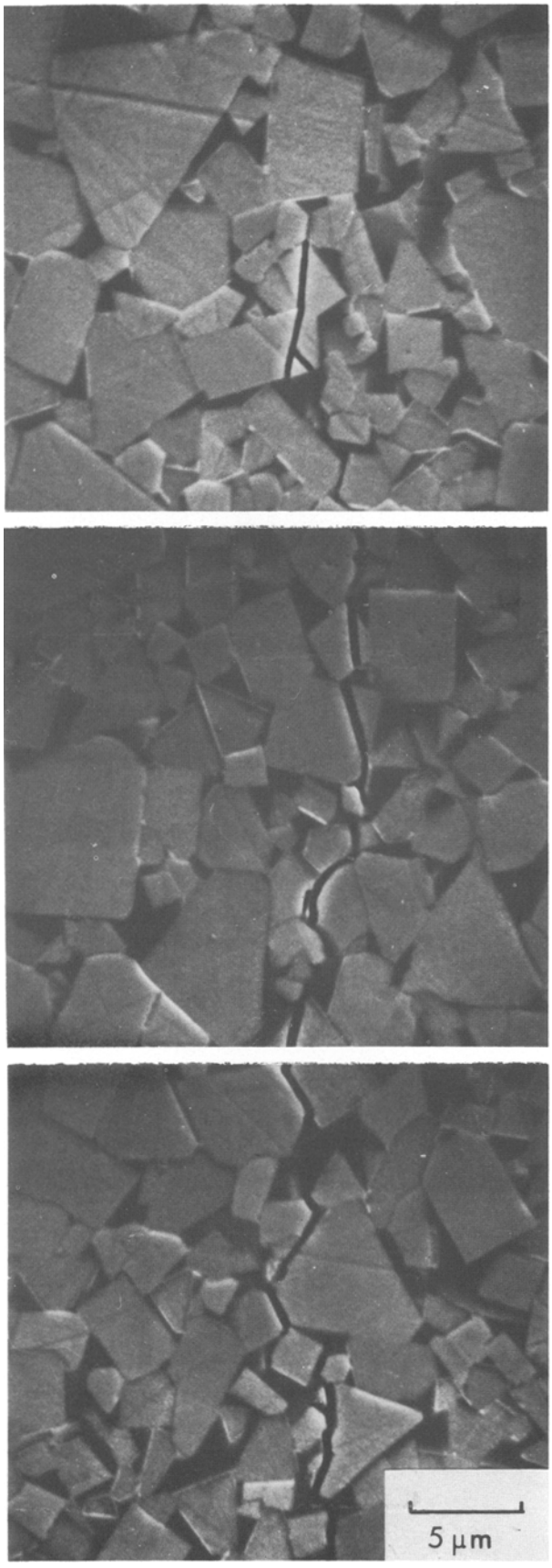

Figure 12 Fatigue fracture path in coarse grained hardmetal G10 (WC–10Co).

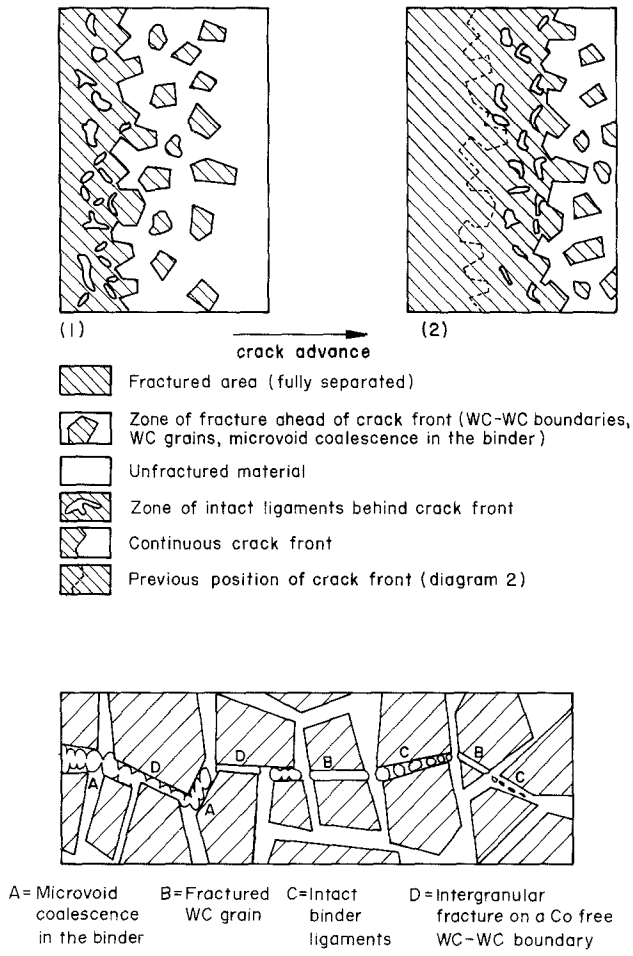

Figure 13 Schematic illustration of the fracture process in WC–Co hardmetals: (a) in the plane of the crack; and (b) in cross-section through the crack front perpendicular to the plane of the crack.

are found as K_{max} approaches the K value at which crack growth under monotonic loading (or "static fatigue") occurs, found to be $\sim 0.9 K_{Ic}$ for these materials.

4. The absence of a frequency effect, together with an analytical comparison of data obtained from monotonic and cyclic crack growth tests, confirms the occurrence of a "true" fatigue process in these materials.

5. Fractographically, fatigue fracture surfaces are indistinguishable from those obtained during "fast" fracture; fracture is primarily intergranular, with ductile rupture occurring in the cobalt binder phase, but with carbide grain cleavage also commonly in evidence.

6. An increasing mean free path in the cobalt phase (increased cobalt content, increased grain size) results in a decreased fatigue crack growth rate; the growth rate exponent m also varies closely with the mean free path.

7. Experimental observations can be adequately interpreted in terms of a model for fatigue crack advance based on the mechanical behaviour, under cyclic loading, of intact binder ligaments interspersed amongst debonded grain boundaries, fractured carbide grains and ruptured binder in the rather ill-defined crack tip region of a propagating fatigue crack.

Acknowledgement

The authors gratefully acknowledge the valuable input of Dr R. B. Tait in the preparation of this manuscript.

References

1. P. M. BRAIDEN, R. W. DAVIDGE and R. AIREY, *J. Mech. Phys. Sol.* **25** (1977) 257–268.
2. F. OSTERSTOCK, Thesis Université de Caen, Caen, France (1980).
3. H. E. EXNER, *Int. Met. Rev.* **243** (4) (1979), 149.
4. K. MIYAKE, Y. FUJIWARA and K. NISHIGAKI, *Nippon Kinzoku Gakki-Shi* **32** (1968) 1128.
5. V. K. SARIN and T. JOHANNESSON, *Metal Sci.* **9** (1975) 472.
6. T. J. DAVIES and S. BARHANA, *Planseeberichte Pulvermetallurgie* **20** (1) (1972).
7. I. JOHANSSON, G. PERSSON and R. HILTSCHER, *Powder Metall.* **13** (1970) 449.
8. A. G. EVANS and M. LINZER, *Int. J. Fracture* **12** (1976) 217.
9. R. C. LUETH, *J. General Electric Eng. Mater. Mater. Technol.* Spring (1981) 27.
10. E. A. ALMOND and B. ROEBUCK, *Metals Technol.* **7** (1980) 83.
11. R. K. VISWANADHAM, personal communication (November 1981).
12. L. LINDAU, "Fracture 1977" ICF4, Vol. 2, edited by D. M. R. Taplin (University of Waterloo Press 1977) pp. 215–21.
13. R. C. LUETH, "Fracture Mechanics of Ceramics", Vol. 2, edited by R. C. Bradt, D. P. H. Hasselman and F. F. Lange (Plenum, New York, 1974) pp. 781–806.
14. J. L. CHERMANT and F. OSTERSTOCK, *J. Mater. Sci.* **11** (1976) 1939.
15. M. NAKAMURA and J. GURLAND, *Metall. Trans.* **11A** (1980) 141.
16. R. K. VISWANADHAM, T. S. SUN, E. F. DRAKE and J. A. PECK, *J. Mater. Sci.* **16** (1981) 1029.
17. N. INGELSTROM and H. NORDBERG, *Eng. Fract. Mech.* **6** (1974) 597.
18. H. E. EXNER and H. F. FISCHMEISTER, *Prakt. Metallogr.* **3** (1967) 18.
19. J. GURLAND, *Trans. AIME* **215** (1959) 601.
20. H. E. EXNER, *Powder Metall.* **13** (1970) 429.
21. H. C. LEE and J. GURLAND, *Mat. Sci. Engng* **33** (1978) 125.
22. G. S. KREIMER, I. I. SIDORIN and E. F. TISHCHENKOVA, *Isv. Akad. Nauk SSSR Otd. Tekhn. Nauk* **3** (1958) 113.
23. P. R. FRY and G. G. GARRETT, "Proceedings International Conference on Recent Developments in Speciality Steels and Hard Materials" (Materials Development '82), Pretoria, R.S.A., edited by N. R. Comins and J. B. Clark (Pergamon, New York, 1982) pp. 375–81.
24. N. KNEE and W. J. PLUMBRIDGE, "Proceedings 6th International Conference on Fracture", Vol. 4, edited by S. R. Valluri, D. M. R. Taplin, P. Rama Rao, J. F. Knott and R. Dubey (Pergamon, 1984) pp. 2685–92.
25. P. R. FRY, MSc dissertation, University of the Witwatersrand, Johannesburg (1982).
26. A. G. EVANS, "Fracture Mechanics of Ceramics", Vol. 1, edited by R. C. Bradt, D. P. H. Hasselman and F. F. Lange (Plenum, New York, 1974) pp. 17–48.
27. J. O. OUTWATER and D. J. JERRY, "On the Fracture Energy of Glass", Interim Report, Contract NONr. 3219 (01) (X), University of Vermont, Burlington, Vermont (August 1966).
28. B. J. PLETKA, E. R. FULLER and B. G. KOEPKE, in "Fracture Mechanics Applied to Brittle Materials", ASTM STP 678, edited by S. W. Freiman (American Society for Testing and Materials, Philadelphia, Pennsylvania, 1979) pp. 19–37.
29. D. P. WILLIAMS and A. G. EVANS, *J. Test. Eval. JTEVA* **1** (1973) 264.
30. R. B. TAIT, P. R. FRY and G. G. GARRETT, *Exp. Mech.* **27** (1987) 14.
31. E. R. FULLER, in "Fracture Mechanics Applied to Brittle Materials", ASTM STP 678, edited by S. W. Freiman (American Society for Testing and Materials, Philadelphia, Pennsylvania, 1979) pp. 3–18.
32. R. K. VISWANADHAM, personal communication (April 1982).
33. J. S. NADEAU, *J. Amer. Ceram. Soc.* **57** (1974) 303.
34. A. G. EVANS, L. R. RUSSELL and D. W. RICHERSON, *Met. Trans.* **6A** (1975) 707.
35. A. G. EVANS and E. R. FULLER, *ibid.* **5** (1974) 27.
36. G. G. GARRETT and J. F. KNOTT, *ibid.* **6A** (1975) 1663.
37. R. O. RITCHIE and J. F. KNOTT, *Acta Metall.* **21** (1973) 639.
38. A. G. EVANS, *Int. J. Fracture* **16** (1980) 485.
39. A. G. EVANS, A. H. HEUER and D. L. PORTER, "Fracture 1977", ICF4, Vol. 1, edited by D. M. R. Taplin (University of Waterloo Press, 1977) pp. 529–56.

Received 28 November 1986
and accepted 22 September 1987